

# A NEW INVESTIGATION ON MECHANICAL PROPERTIES OF FERRO-TITANIT

M. Foller and H. Meyer

*Edelstahl Witten-Krefeld GmbH*

*Sonderwerkstoffe Gladbacher Str. 578*

*D-47805 Krefeld*

*Germany*

**Abstract** Besides high resistance against abrasion a wear resistant material has, depending on the application, to fulfil many other demands. Toughness, corrosion resistance, stiffness or damping properties are only a small selection out of many specific requirements. In this paper mechanical properties of different grades from the Ferro-Titanit material group are investigated to get a better understanding of the material behaviour in use and a decision support for material selection for special applications. Bending fracture strength, modulus of elasticity and shear, Poisson values and velocity of sound are determined under consideration of material composition and heat treatment. Ferro-Titanit are machinable and hardenable alloys containing up to 45 % by volume Titanium Carbide (TiC) embedded in an alloyed steel binder phase. The high amount of carbides requires powder metallurgical methods of production. A choice can be made out of seven different steel grades which can be classified into three groups with carbon martensitic, nickel martensitic and austenitic binder phases.

**Keywords:** Ferro-Titanit, metal matrix composites, MMC, titanium carbide, TiC, Cermet, modulus of elasticity, Young's modulus, modulus of shear, modulus of compression, Transverse contraction ratio, Poisson value, velocity of sound, fracture behaviour, bending fracture strength

## INTRODUCTION

Depending on the application tools, machine-parts or fittings are subjected to different more or less severe kinds of strain and wear. One of

the most important reasons for wear and failure is abrasion. An effective preventive countermeasure is to increase the hardness of the particular part. This can be done with steel by alloying and special heat treatment to alter the structure and precipitate hard particulates mainly carbides. By conventional smelting technologies the amount of carbides can be increased only to a limited amount so that powder-metallurgical methods have to be applied. This technique allows to create a variety of new steel grades with excellent properties fulfilling extreme demands. A special group among these materials is constituted by the Ferro-Titanit metal matrix composites (MMCs). Ferro-Titanit is steel-bonded titanium carbide (TiC) and can be classified into the material group of Cermets. TiC is a very interesting structure constituent because of its extreme hardness, thermodynamic stability, low density, thermal conductivity and easy availability. Despite the high amount of carbides of up to 45 % vol., Ferro-Titanit can be machined by conventional techniques like sawing, milling, turning or tapping in the soft annealed state. Thereafter it can be hardened up to values of about 70 HRC by a vacuum heat treatment. While for all grades the prime constituent is titanium carbide (TiC), the binder material is either carbon martensitic, nickel martensitic or austenitic steel. Due to variations in alloying content within these groups, depending on the special demands of a certain application, a choice out of seven grades can be made providing a broad variety of properties exceeding excellent abrasion resistance [1, 2, 3]. An overview of the chemical compositions and a classification of the Ferro-Titanit grades in carbon martensitic, nickel martensitic and austenitic binder phases is given in Table 1.

Figure 1 shows a scanning electron micrograph of hardened and tempered WFN. This Ferro-Titanit grade consists of 33% by weight ( $\approx$  45% vol.) of TiC and has a carbon martensitic tool steel based binder phase with about 13.5% Cr. For the micrograph backscattered electrons are detected to get a better mass contrast. The homogeneously dispersed dark grey TiC-particulates imbedded in the steel matrix can be clearly identified. Also a core / shell structure, well known for Cermets [4, 5], can be seen. The core consists of pure TiC while the shell (a degree lighter grey than the core) has additionally a high amount of Mo which diffused during the sintering process into the TiC particulates. Some Cr-rich Carbides can be found mainly bridging TiC particulates. The steel binder phase shows a regular martensitic structure.

Table 1. Composition of the different Ferro-Titanit grades, main components

Structure of the matrix	grades	carbide content TiC	chemical composition of the steel matrix [%] by weight					
			C	Cr	Co	Mo	Ni	Fe
carbon martensite	C - Spezial	33.0	0.65	3.0		3.0		Bal.
	WFN	33.0	0.75	13.5		3.0		Bal.
	S	32.0	0.50	19.5		2.0		Bal.
nickel martensite	Nikro 128	30.0		13.5	9	5.0	4.0	Bal.
	Nikro 143	30.0			9	6.0	15.0	Bal.
austenite	Cromoni	22.0		20.0		15.5		Bal.
	U	34.0		18.0		2.0	12.0	Bal.

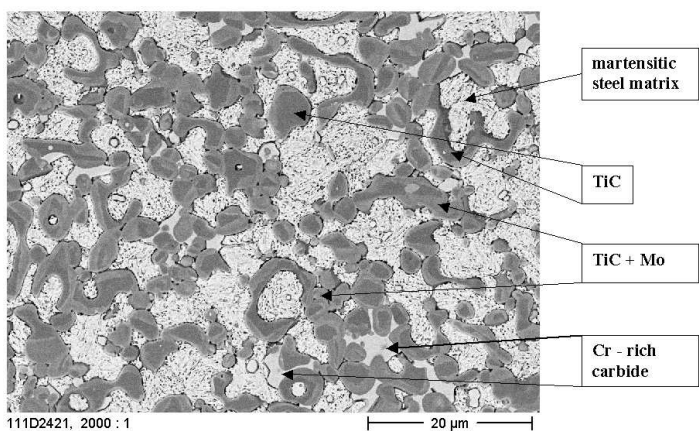


Figure 1. Scanning electron micrograph of WFN, hardened and tempered, backscattered electrons (mass contrast).

In this paper mechanical properties of different grades from the Ferro-Titanit material group are investigated to get a better understanding of the material behaviour in use and a decision support for material selection for special applications. Measuring velocity of sound allows a calculation of mechanical properties like modulus of elasticity, compression and shear modulus and Poisson values. Beside this the bending fracture strength was determined. The tests have been done under consideration of material com-

position and heat treatment. Additional investigations concerning the fracture behaviour of Ferro-Titanit are performed.

## TEST METHOD

### ELASTIC PROPERTIES

Mechanical properties of a solid-state body like modulus of elasticity, Poisson value or modulus of compression can be determined by the ultrasonic pulse-echo procedure [6, 7]. By measuring the transition time of the transversal and the longitudinal waves together with the sample thickness and the density, characteristic material values can be calculated as follows:

$$E = 2G(1 + \mu) \quad (1)$$

$$G = \rho \frac{d^2}{t_L^2} \quad (2)$$

$$\mu = \frac{t_T^2 - 2t_L^2}{2(t_T^2 - t_L^2)} \quad (3)$$

$$K = \frac{E}{3(1 - 2\nu)} \quad (4)$$

$$c_T = \frac{d}{t_T} \quad (5)$$

$$c_L = \frac{d}{t_L} \quad (6)$$

$E$ : modulus of elasticity (Young's modulus),  
 $\rho$ : density,  
 $G$ : modulus of shear,  
 $\mu$ : transverse contraction ratio (Poisson value),  
 $K$ : modulus of compression,  
 $c_T$ : velocity of sound transversal,  
 $c_L$ : velocity of sound longitudinal,  
 $t_T$ : transit time transversal,  
 $t_L$ : transit time longitudinal,  
 $d$ : sample thickness.

For each material condition three samples have been measured and the mean value is stated in the diagrams and tables below. The measurements have been performed at the Technical University of Dresden.

## FRACTURE BEHAVIOUR

Because of the high amount of hard phases in Ferro-Titanit, the fracture behaviour is more comparable with hard metal than with steel. For this reason the bending fracture strength is determined according to standard DIN ISO 3327 [8] for hard metals with a three point bending test. Following the standard, samples with shape A (dimension  $35 \times 5 \times 5$  mm) and a phase of 0.15–0.2 mm were used. The surfaces of the samples were ground with diamond. The load was induced by a roll.

The bending fracture results from the equation:

$$R_{bm30} = \frac{3Fl}{2bh^2} \quad (7)$$

$F$ : force which is necessary to break the sample,

$l$ : distance of support rolls

$h$ : height of sample

$b$ : width of sample

$R_{bm30}$ : bending fracture measured with  $l = 30$  mm

Bending fracture tests have been performed at the Fraunhofer Institute Manufacturing Advanced Materials in Dresden. For each material condition ten samples have been tested and the mean value and the respective standard deviation are stated. To get more information on the fracture behaviour of Ferro-Titanit broken samples have been inspected by a field emission scanning electron microscope (FE-SEM) at the Research Institute of Thyssen Krupp Steel in Duisburg / Hamborn.

## TEST RESULTS

### ELASTIC PROPERTIES

In Table 2 all test results of the different Ferro-Titanit grades in the soft and hardened condition are summarized. A C-Spezial – variant with a lower TiC-content of 23% has additionally been tested. The hardness values of the different heat treatment conditions are also stated.

In Fig. 2a, 2b the modulus of elasticity  $E$  (Young's modulus) is shown in a diagram. While  $E$  is between 300 and about 310 GPa for the carbon martensitic grades and Nikro 128 and U have only slightly lower values, Nikro 143 and Cromoni show a value which is distinctly smaller. Remarkably is that

Table 2. Velocity of sound and elastic properties of Ferro-Titanit

grade	status of heat treatment	hardness [HRC]	$c_L$ [m/s]	$c_T$ [m/s]	$E$ [GPa]	$G$ [GPa]	$K$ [GPa]	$\mu$	$R_{bm30}$ [GPa]
C-Spezial	soft annealed	50	7540	4370	308	123	202	0,247	1578
C-Spezial	hardened and tempered	69	7420	4290	303	121	201	0,248	1803
C-Spezial, 23%TiC	soft annealed	43	7060	4040	278	111	191	0,257	1677
C-Spezial 23%TiC	hardened and tempered	64	6930	3940	269	107	187	0,261	2146
WFN	soft annealed	50	7610	4470	312	126	198	0,237	1255
WFN	hardened and tempered	68	7460	4320	299	120	199	0,249	1621
S	soft annealed	50	7520	4400	308	124	198	0,241	1208
S	hardened and tempered	66	7450	4310	302	121	200	0,248	1279
Nikro 128	solution annealed	50	7310	4260	295	119	192	0,244	1367
Nikro 128	age hardened	62	7370	4290	298	120	194	0,244	1281
Nikro 143	solution annealed	51	7140	4070	276	110	192	0,261	1453
Nikro 143	age hardened	62	7190	4130	284	113	192	0,254	1627
Cromoni	solution annealed	52	6920	3880	279	110	202	0,270	1294
Cromoni	age hardened	56	6950	3910	284	112	204	0,268	1443
U		48	7330	4280	296	120	190	0,241	1156

for the carbon martensitic grades the E value is always slightly higher in the soft annealed state, while with the other grades the modulus of elasticity is slightly higher in the age hardened state. It should be expected that a material has a higher modulus of elasticity with rising hardness as it can be seen with the age hardened grades Nikro 128, Nikro 143 and Cromoni. Probably the unexpected behaviour of the carbon martensitic grades arises, together with having a composite material, from the change of structure during the hardening process, while during age hardening with Nikro grades and Cromoni only precipitation occurs. Since the elastic properties are calculated from the velocity of sound of the transversal and longitudinal waves, the different behaviour of the two material groups can already be found directly in the basic data  $c_T$  and  $c_L$  (Figs. 3a and 3b) and also in the other derived properties like the Poisson values (Figs. 4a and 4b).

For special applications it is noticeable that the velocity of sound is altered by the hardening process. This is very important e.g. for the lay out of tools for ultrasonic processing so called sonotrodes. Here the velocity of sound is essential for the calculation of the dimensions of this kind of tools. The carbon martensitic grades have a lower velocity of sound after hardening while the nickel martensitic grades and the austenitic Cromoni show a slightly higher velocity of sound. However the change of the latter group by the heat treatment procedure is tendentially smaller.

## **BENDING FRACTURE STRENGTH AND FRACTURE BEHAVIOUR**

Table 2 and Figs. 5a and 5b show the bending fracture strength of all Ferro-Titanit grades in the soft and hardened state. Within the group of carbon martensitic binder phases (Fig. 5a) the grade C-Spezial has the highest bending fracture strength then followed, with rising chromium content, by the grades WFN and S. With the exception of Nikro 128 and the austenitic U all grades have a higher strength in the hardened state. The highest strength is measured with C-Spezial in the hardened state with reduced TiC content.

In Fig. 6 bending vs. load plots of the C-Spezial variants are shown. As well as the ordinary and the TiC-reduced material exhibit in the hardened state nearly no plastic deformation which is revealed by the nearly exact linearity of the graph following Hook's law. On the other hand in the soft annealed state even with 33 % TiC there is a slight plastic deformation which

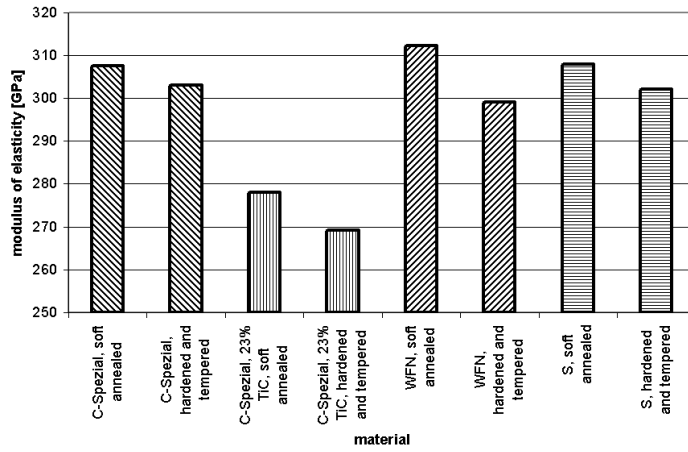


Figure 2a. Modulus of elasticity of Ferro-Titanit with carbon martensitic binder phase, hardened and soft annealed.

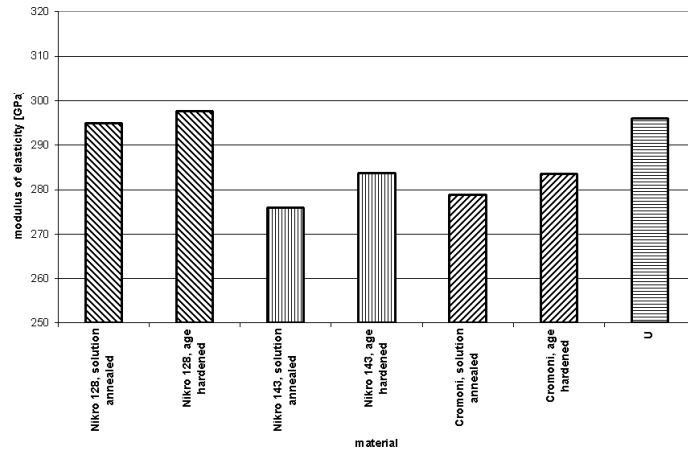


Figure 2b. Modulus of elasticity of Ferro-Titanit with nickel martensitic and austenitic binder phase, solution annealed and age hardened.

is drastically larger with 23 % TiC. The lack of nearly any plastic deformation of the hardened matrix confirms the experience that straightening after hardening of Ferro-Titanit is not possible.



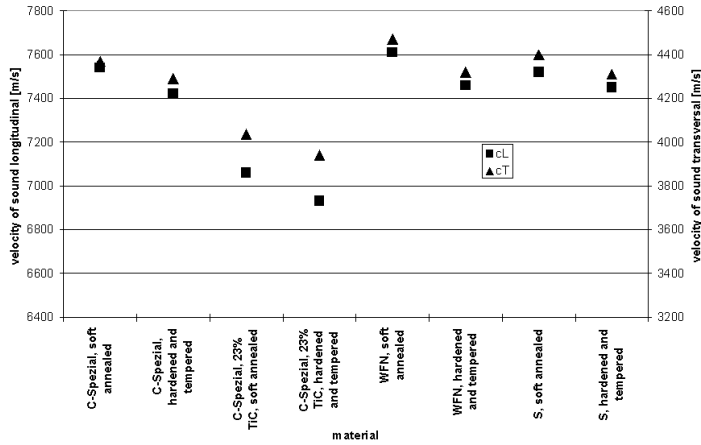


Figure 3a. Velocity of sound longitudinal and transversal of Ferro-Titanit with carbon martensitic binder phase, hardened and soft annealed.

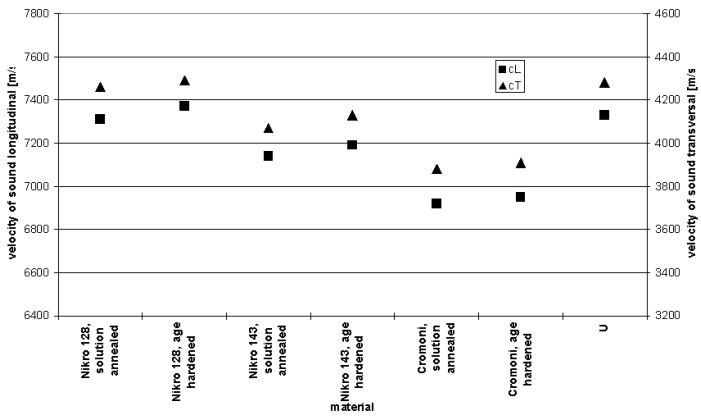


Figure 3b. Velocity of sound longitudinal and transversal of Ferro-Titanit with nickel martensitic and austenitic binder phase, solution annealed and age hardened.

In Figs. 7 and 8 the fracture surfaces of WFN in the soft annealed condition and the hardened and tempered state are shown. While the soft material shows a coarse grained appearance of fracture the hardened material appears more fine grained and brittle. Noticeable is that in the fracture plane nearly all TiC particles are cleaved. Only very few undamaged particles can be

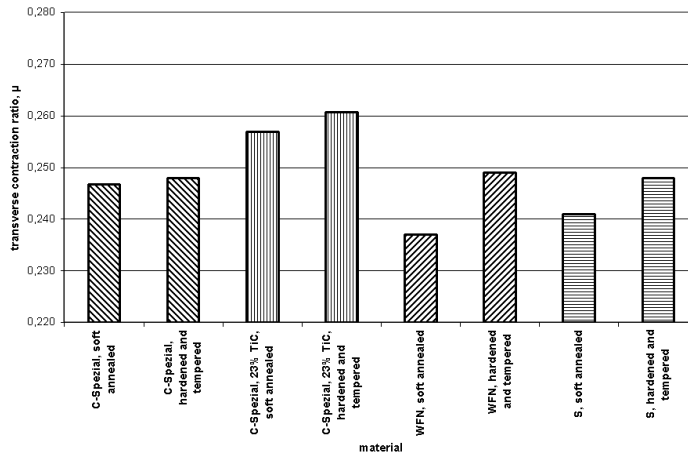


Figure 4a. Transverse contraction ratio of Ferro-Titanit (Poisson value) with carbon martensitic binder phase, hardened and soft annealed.

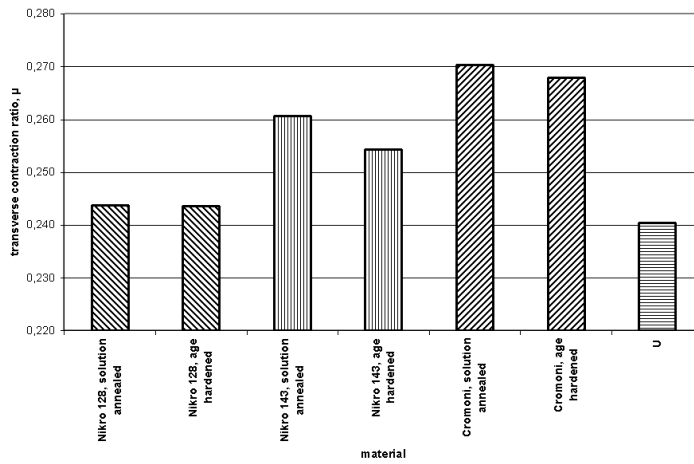


Figure 4b. Transverse contraction ratio of Ferro-Titanit (Poisson value) with nickel martensitic and austenitic binder phase, solution annealed and age hardened.

found (Fig. 9) proving the excellent bonding between TiC-particulates and steel matrix. Mainly in the soft state, areas can be found where the matrix

shows a tough deformed fracture structure of the steel, reflecting the plastic behaviour shown in Fig. 6.

A cross section perpendicular to the fracture surface gives a good insight into the fracture mechanism of Ferro-Titanit. Near the fracture plane single TiC particles can be found with isolated cracks like shown in Fig. 10. The direction of the cracks are more or less parallel to the fracture surface i.e. perpendicular to the forces arising during the bending test. Ferro-Titanit is a metal matrix composite (MMC) of steel with a relatively low E-modulus of about 190 GPa [9] reinforced by ceramic TiC particulates with a high E-Modulus of 470 GPa [10]. Taking this into consideration, it can be expected that under tensile load stress peaks arise in the stiffer and more brittle carbide phases, especially if there is a strong bonding between the hard phase and the more ductile binder phase. The consequence is obviously that the initial material failure occurs in the TiC by cleaving the particles (Fig. 10). This initial crack can be stopped first if it runs out in surrounding ductile steel binder phase.

The propagation of cracks predominantly follows, if possible, through adjacent TiC particulates. Figure 11 and Fig. 12 show propagated cracks near the fracture surface. Cracks can still be stopped by the ductile binder phase (Fig. 11), or go straight through the hard binder phase to bridge gaps between particles with a slightly higher distance (Fig. 12). The fine grained structure of the fracture plane in Fig. 8 can be explained with the lower toughness of the hardened steel matrix. A crack initiated in a TiC particulate can more easily propagate directly through the hardened binder phase while in the soft annealed state cracks predominantly follow the TiC particles.

A comparison of the bending and fracture behaviour of C-Spezial with 33 % and 23 % TiC (Fig. 5a and Fig. 6) shows that with a lower TiC content a considerably stronger bending and higher bending fracture strength can be achieved. This can be explained by the larger mean distance between hard phase particles preventing more effective cracks from propagating from one particulate to the next.

## **SUMMARY**

Velocity of sound of transversal and longitudinal waves has been measured for all Ferro-Titanit grades in the soft annealed and hardened condition. Elastic properties like E-modulus, shear modulus and Poisson values were calculated from the measured velocity of sound values. The bending fracture

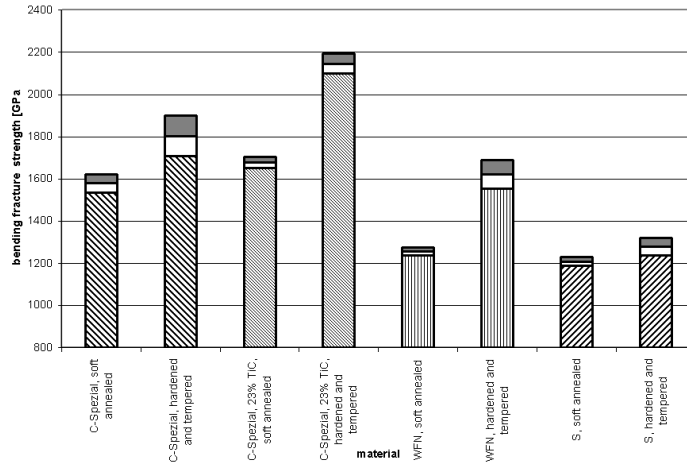


Figure 5a. Bending fracture strength of Ferro-Titanit with carbon martensitic binder phase, hardened and soft annealed.

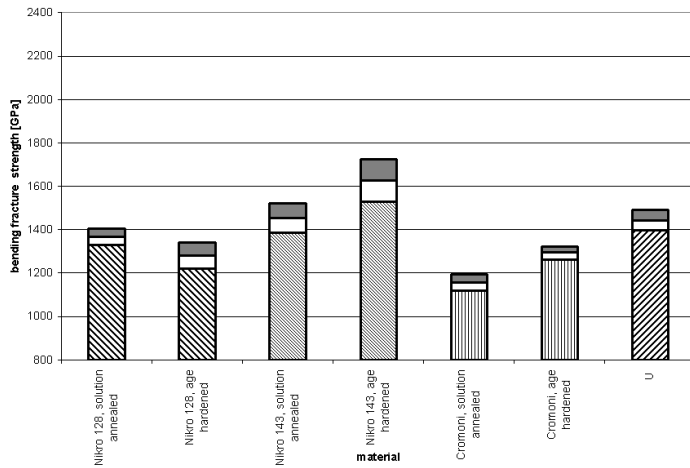


Figure 5b. Bending fracture strength of Ferro-Titanit with nickel martensitic and austenitic binder phase, solution annealed and age hardened.

strength was measured and the elastic and plastic parts were discussed. In the hardened condition practically no plastic deformation can be detected even with reduced amount of hard phase. Under tensile stress, initial material

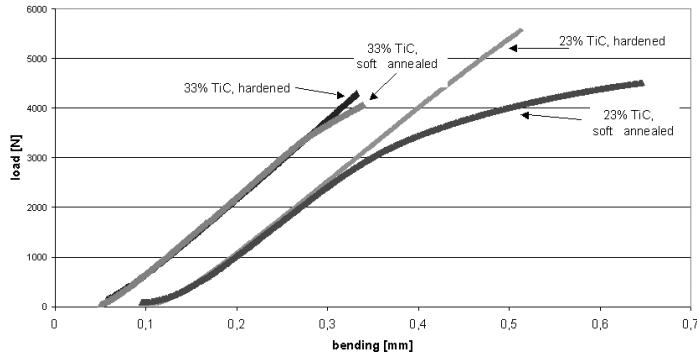


Figure 6. Bending as a function of load, C-Spezial with reduced TiC content (23 %) and usual TiC content (33 %) both variants soft annealed and hardened; positions of the curves are shifted.

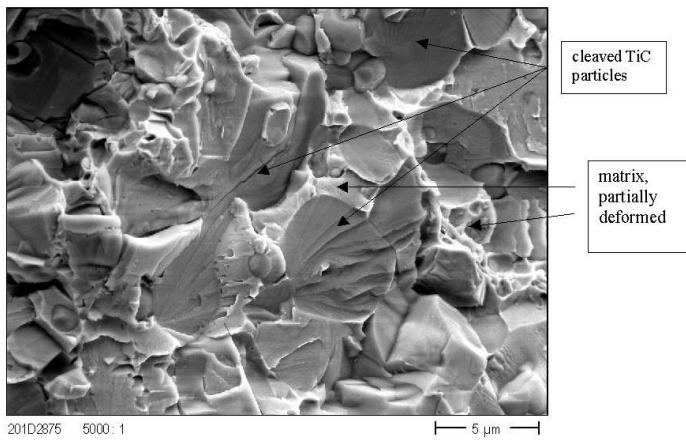


Figure 7. Fracture surface of WFN, soft annealed.

failure occurs by cleaving single TiC particulates. Crack propagation predominantly follows through adjacent hard phase particulates. In the fracture surface only few uncleaved TiC particles can be found proving the excellent bonding between steel binder phase and hard phase.

**REFERENCES**

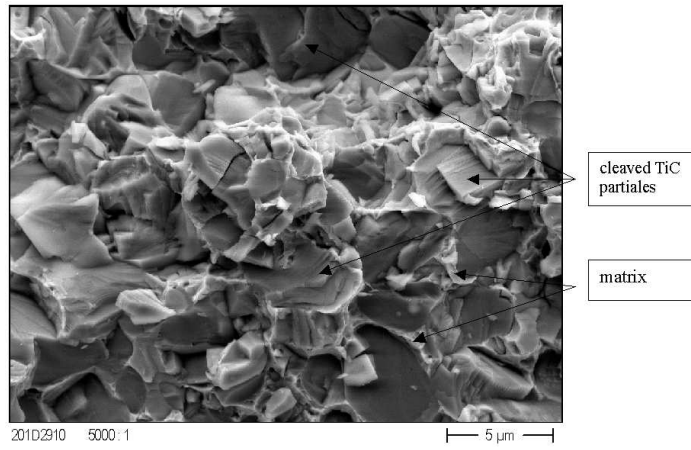


Figure 8. Fracture surface of WFN, hardened and tempered.

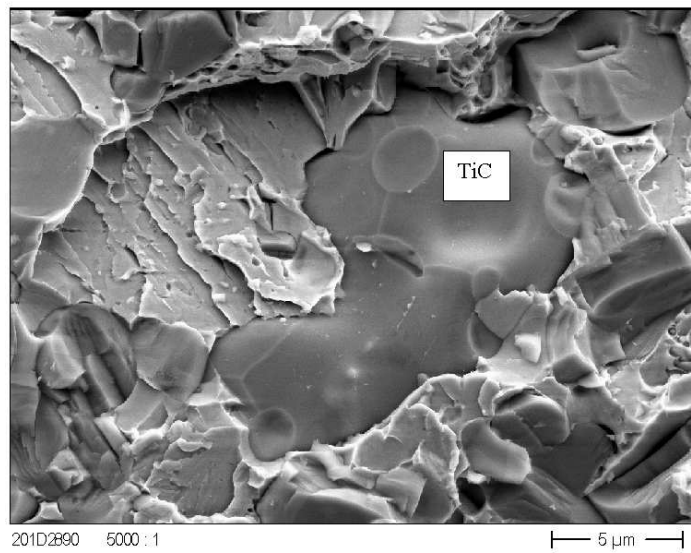


Figure 9. Fracture surface of WFN, soft annealed, undamaged TiC particle.

- [1] U. DRAUGELATES, M. FOLLER, M. GROSS, H. MEYER, R. REITER "An Investigation on Wear caused by Cavitation on Ferro-Titanit", Proceedings on the Interna-

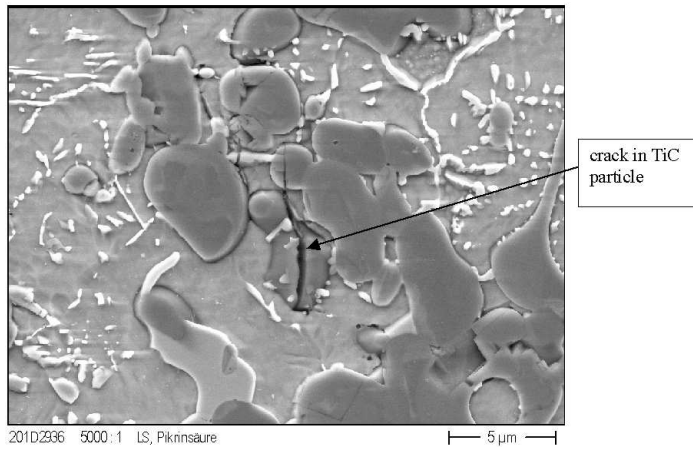


Figure 10. FE-SEM picture of WFN soft annealed near the fracture with crack in TiC particle.

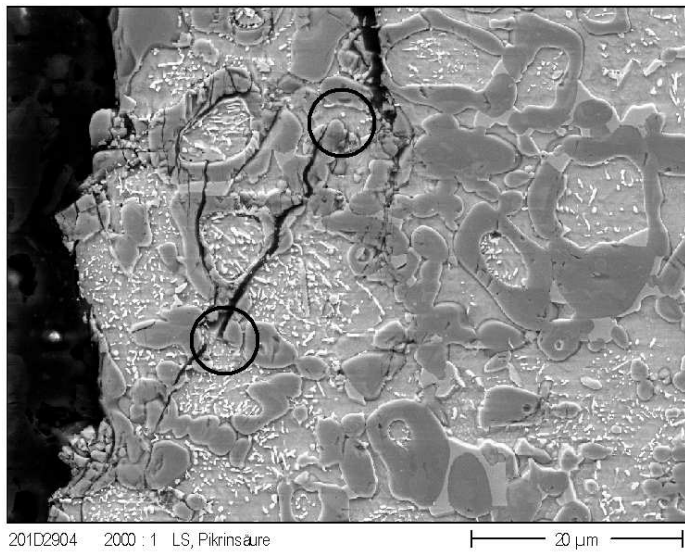


Figure 11. FE-SEM picture of WFN soft annealed near the fracture surface, cracks following TiC particulates stopped by the ductile binder phase (e.g. marked by circles).



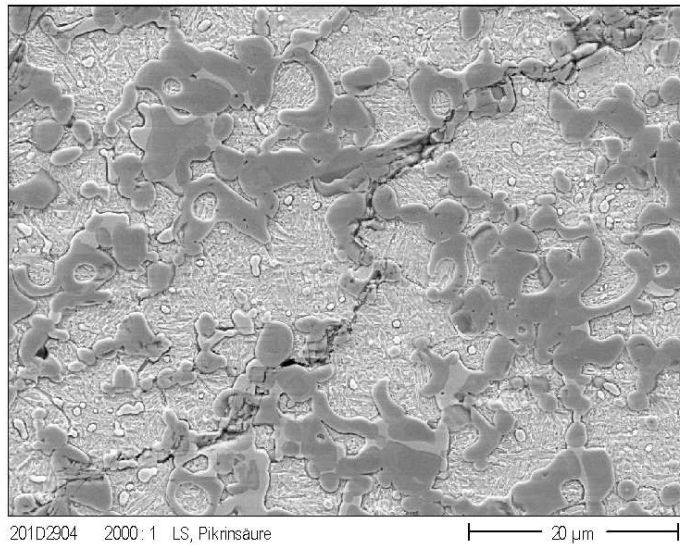


Figure 12. FE-SEM picture of WFN hardened. near the fracture with a crack line.

tional conference on Powder Metallurgy and Particulate Materials"; June 2000 New York

- [2] M. FOLLER, H. MEYER, L. SCHNEIDER; "Gleitverschleißuntersuchungen unter Einwirkung körniger Stoffe an Werkzeugwerkstoffen vom Typ FERRO-TITANIT" Proceedings zum Symposium Reibung und Verschleiß, 6.-7. April 2000 in Bad Nauheim
- [3] M. FOLLER, A. LAMMER, H. MEYER, "Wear and Corrosion of Ferro-Titanit and Competing Materials", Proceedings 5th International Conference on Tooling, 29.9.–1.10.99 in Leoben Austria
- [4] H.-O. ANDREN, U. ROLANDER and P. LINDAHL, "Phase Composition in Cemented carbides and Cermets", Proceedings of the 13th International Plansee Seminar Vol. 2 Reutte (1993) p. 1–15
- [5] M. EHIRA, A. EGAMI, "Mechanical Properties and Microstructures of Submicron Cermets", Proceedings of the 13th International Plansee Seminar Vol. 2 Reutte (1993) p. 16–25
- [6] V. DEUTSCH, M. PLATTE and M. VOGT, in "Ultraschallprüfung" (Springer, Berlin 1997) p. 313 pp
- [7] F. BERGNER, Seminarunterlagen "Zerstörungsfreie Materialcharakterisierung" Jena 996, (Deutsche Gesellschaft für zerstörungsfreie Prüfung) p 109



- [8] DIN ISO 3327, "Bestimmung der Biegebruchfestigkeit" 1991-07
- [9] Datasheet of tool steel X 155 CrVMo 12 1 (1.2379), Edelstahl Witten-Krefeld GmbH
- [10] H. HOLLECK, J.Vac. Sci. Technol., Vol. 4, No. 6, Nov/Dec 1986, p. 2661–2669